Proceedings of the 5th International Conference on Computing and Data Science
DOI: 10.54254/2755-2721/20/20231076

QUAV attitude control based on linear active disturbance rejection control

Xianming Li[1], Jiabo Tong[2,4], and Haotian Zhu[3]

[1]School of Electrical and Electronic Engineering, Wuhan Polytechnic University, Wuhan, China
[2]School of Energy and Power Engineering, Wuhan University of Technology, Wuhan, China
[3]School of Advanced Manufacturing, Guangdong University of Technology, Guangzhou, China

[4]299493@whut.edu.cn
All the authors contributed equally, and their names were listed in alphabetical order.

Abstract. Unmanned Aerial Vehicle (UAV) are currently gaining popularity. This paper proposes a method to apply Linear Active Disturbance Rejection Control (LADRC) to Quadrotor Unmanned Aerial Vehicle (QUAV) controller to optimize the traditional PID controller. Firstly, the application and shortcomings of traditional PID control in UAV are introduced, and the LADRC method is proposed. Then linear simplification and Parameter Setting of ADRC are carried out. In the Simulink environment, according to the mathematical model of the QUAV, a QUAV dynamics simulation platform is established. Finally, according to different control channels, different control algorithms are designed, and tracking models are introduced in various attitudes to simulate and verify the control effect of LADRC. The results show that the LADRC controller is effective, the LADRC can be effectively combined with the traditional PID control. The application in the QUAV can realize more precise QUAV speed tracking control and the stable flight of the QUAV. Compared with the traditional PID controller, under the experimental conditions of this paper, the LADRC controller has more precise control accuracy and more efficient control efficiency. Finally, this paper summarizes the design of LADRC and makes a brief outlook on the development of UAVs.

Keywords: PID control, QUAV, LADRC, parameter tuning, UAV dynamics.

1. Introduction

With the advent of the era of information technology, efficient and convenient drones have become special aircraft that can be applied to various fields, such as medical transportation during the new crown period, urban public security supervision, agricultural management, remote power transmission, optical fiber monitoring, and maintenance, etc. As the Quadrotor Unmanned Aerial Vehicle (QUAV) with the simplest structure, high safety, and strong variability among drones, it is the most widely used in the field of drones. From personal photography to military confrontation, QUAV can be seen usually.

QUAV has developed rapidly in recent years. QUAV are usually composed of batteries, controllers, motors, propellers, sensors, and some additional components, including cameras, robotic arms, and other

DOI: 10.54254/2755-2721/20/20231076

components customized according to users. QUAV has multiple inputs: such as lift, airflow, gravity, etc. Multiple outputs: such as yaw angular velocity, pitch angular velocity, roll angular velocity, etc. And it is an under-coupled system [1]. Therefore, the controller design of the QUAV is particularly important, which is related to the safe flight and economical reliability of the UAV. For the control of QUAV, the traditional method is to use the PID control algorithm [2]. The PID algorithm is simple in design, mature in technology, and has applications in a variety of long-span fields. It has become the mainstream control algorithm for drones in the early years. However, since the PID control algorithm is based on the compensation of the error between the given value and the measured value, although it has a certain dynamic performance, it cannot achieve fast and accurate performance when the environment is complex, or the control mode is switched quickly when there has strong interference. Some other control methods are proposed. Robust control methods are mostly used to improve the anti-disturbance optimization of traditional PID control [3]. The common method is robust PID control based on signal compensation. The application of this method does not require complex design and the robust PID can be used in other areas of control technology.

The linear quadratic (LQR) control linearizes the QUAV model and obtains the closed-loop optimal control under the optimal condition of the performance function [4]. However, this method is not suitable for some strong nonlinear situations, such as large-angle steering or roll control. To solve this problem, a variable structure control strategy in which the control quantity can be switched with the state is proposed [5]. The influence of model parameters and disturbances on the control method will be greatly reduced, and the system will obtain better robustness. The control method based on neural networks and fuzzy strategy is a new method in the research field of QUAV control in recent years, but some problems of engineering experience and design difficulty still exist [6, 7]. To overcome the difficulties of engineering experience, an L1 Adaptive Controller for State Feedback and Output Feedback by Projection Operator Adaptive Law and Piecewise Constant Adaptive Law was designed [8]. Theoretical reasoning shows that the L1 Adaptive Controller can realize fast and stable control on the QUAV under the influence of model parameter perturbation and external disturbance. However, this research lacks practical application.

Comparing different control strategies, this paper proposes a linear active disturbance rejection control method combined with modern control theory, which is combined with PID control and optimized. To verify the feasibility of the method, a QUAV dynamic model is established, which fully considers the dynamics of the QUAV and can realize trajectory visualization. A perturbation signal is added to simulate the control stability of the QUAV under external disturbance. The performance of the simulation model is validated and the effect of the LADRC control method is verified by simulation.

The main contributions of this paper are as follows:

1) Establishment of QUAV dynamic model with target setting control flight.

2) Optimization of PID control algorithm and design of LADRC control.

3) Based on LADRC, the performance evaluation is made, and future UAV research has prospected.

2. Problem formulation

As one of the most classical control algorithms, PID is widely used in the sector of industrial control due to its simple structure, excellent stability, and convenient adjustment. The PID algorithm can act out a good performance of control by adjusting parameters even if the exact structure and mathematical model of the controlled object cannot be obtained. The theory is to make a difference according to the setting expectant and actual output value of the system and adjust deviation by use of proportional, integral, and differential control. Its structure is shown in Figure 1.

DOI: 10.54254/2755-2721/20/20231076

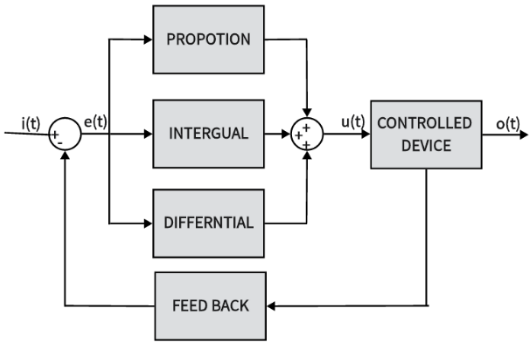

Figure 1. PID control block diagram.

The PID algorithm is primarily used to compensate for the error between the expectant and the output value [9]. The PID system is composed of proportional link, differential link, and integral link. The feedback forms a closed loop with the feedback unit. The expression of the PID control algorithm can be written as:

$$u(t) = K_p \left[e(t) + \frac{1}{T_i} \int_0^t e(t)\, dt + T_d \frac{de(t)}{dt} \right] \tag{1}$$

In the equation above, K_p represents the proportional time coefficient,T_i represents the integration time coefficient,T_d represents the differential time coefficient,u(t) represents the output signal,e(t) represents the input signal.

According to the above equation, it can be concluded that system transfer equation is:

$$G(s) = \frac{u(s)}{e(s)} = K_p \left(1 + \frac{1}{T_i s} + T_d s \right) \tag{2}$$

To facilitate the processing of digital signal circuits, the output response relationship equation can be obtained after discretizing continuous variables:

$$\begin{cases} e(t) = e(k) - e(k-1) \\ u(t) = K_p e(t) + K_i \int e(t)dt + K_d \frac{de}{dt} \end{cases} \tag{3}$$

In this equation, t is the sampling period,K_P,K_i,K_d are respectively the proportional coefficient, integral coefficient, and derivative coefficient. The performance of the controller is closely related to the selection of these three parameters.

The design of a PID controller is relatively simple, but the control effect depends on the selection of parameters. Proper parameter selection can make the system reach a steady state with no overshoot or small overshoot in a short time. However, inappropriate parameters will cause the system to oscillate or diverge.

The proportional link K_P is the simplest control link. According to Equation (3), the output value of the controller u(t) is proportional to the error e(t), so the larger the proportional coefficient, the faster the response can be made, and the deviation can be reduced. However, if the parameter of proportions is too large, the overshoot will increase, and the system will become unstable. At the same time, using only proportional regulation, the system cannot eliminate the steady-state error.

The integration link K_i is used to eliminate the steady-state error of the system. The output value u(t) is proportional to the error e(t) integral. As time increases, the integral term will also increase, making the steady-state error continuously decrease until it is equal to zero. The larger the value of K_i, the faster the elimination of the steady-state error, but at the same time, it will cause integration saturation, reduce the response speed, and increase the modulation.

K_d reflects the change rate of the error in the recent period. By predicting the changing trend of the error in the future, an effective correction signal is introduced in advance, which plays the role of advanced regulation. The adjustment time and overshoot of the system can be reduced if K_d is selected appropriately, but the differential magnifies the noise, and the anti-interference performance of the system will be weakened if K_d is too high.

In general, PID control technology needs to compensate for the error between the expected input and output of the control object, and PID is sensitive to changes in the environment, and it is difficult for some complex nonlinear systems to meet the control requirements.

3. Dynamic model of QUAV

QUAV has four motor-driven rotors. By controlling the rotation of the four motors, it can complete all motion changes of the QUAV, including roll, yaw, and pitch. The purpose of establishing the QUAV model is to analyze the position and attitude changes of the QUAV under the condition of external torque.

3.1. QUAV model principle

QUAV has four motor-driven rotors. By controlling the rotation of the four motors, it can complete all motion changes of the QUAV, including roll, yaw, and pitch. The purpose of establishing the QUAV model is to analyze the position and attitude changes of the QUAV under the condition of external torque.

First, the body coordinates of the UAV are defined, as shown in Figure 2. T represents the lift generated by the UAV, the arrows represent the rotation directions of the four rotors, and d represents the distance between the center of gravity and the propeller.

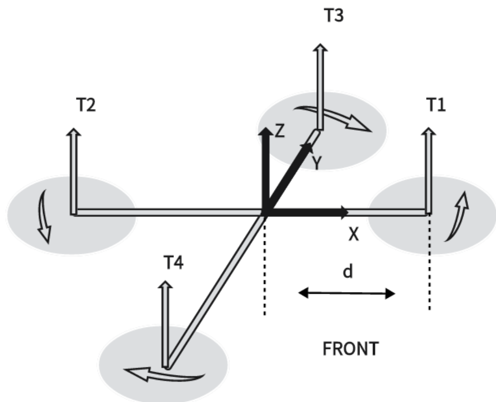

Figure 2. QUAV body coordinate system.

The QUAV is an X-distribution QUAV. The control strategy of this type of UAV is more complicated than that of the traditional cross-type UAV, but its flexibility is stronger than that of the traditional type. The torque generated by the four rotors of the X-type UAV conforms to the right-hand spiral law of physics.

The QUAV model was built with five subsystems, including three mathematical models and two physical models. Its topology is shown in Figure 3. The position dynamic equation is as follows. The position dynamic equation is as follows.

$$\begin{cases} \dot{V}_x = -\frac{f}{m}(cos\psi sin\theta cos\phi + sin\psi sin\phi) \\ \dot{V}_y = -\frac{f}{m}(cos\psi sin\theta cos\phi - cos\psi sin\phi) \\ \dot{V}_z = g - \frac{f}{m}cos\phi cos\theta \end{cases} \tag{4}$$

DOI: 10.54254/2755-2721/20/20231076

It can be seen from the equation that the input is the attitude angle $\phi,\ \theta,\ \psi$, acceleration of gravity, total pull f, and QUAV quality m.

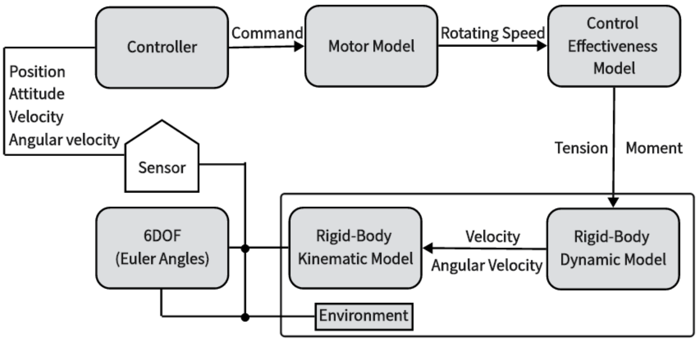

Figure 3. QUAV model topology.

The attitude dynamic equation is as follows.

$$\begin{cases} \dot{p} = \frac{1}{I_{xx}}\left[\tau_x + qr\left(I_{yy} - I_{zz}\right) - J_{RP}q\Omega\right] \\ \dot{q} = \frac{1}{I_{yy}}\left[\tau_y + pr(I_{zz} - I_{xx}) - J_{RP}p\Omega\right] \\ \dot{r} = \frac{1}{I_{zz}}\left[\tau_z + pq\left(I_{xx} - I_{yy}\right)\right] \end{cases} \tag{5}$$

It can be seen from the equation that the input is the anti-torque torque $\tau_x,\ \tau_y,\ \tau_z$ generated by the propeller in the body coordinate system. $I_{yy},\ I_{zz}, I_{zz},\ J_{RP}$ is moment of inertia. p, q, r is the quadrotor angular velocity under the body axis. $\dot{p},\ \dot{q},\ \dot{r}$ is quadrotor angular acceleration. The position kinematics and attitude kinematics equations are as follows.

$$[\dot{x}\ \dot{y}\ \dot{z}]^T = \left[v_x\ v_y\ v_z\right]^T \tag{6}$$

$$\begin{bmatrix} \dot{\phi} \\ \dot{\theta} \\ \dot{\psi} \end{bmatrix} = \begin{bmatrix} 1 & tan\theta sin\phi & tan\theta cos\phi \\ 0 & cos\phi & -sin\phi \\ 0 & sin\phi/cos\theta & cos\phi/cos\theta \end{bmatrix} \times \begin{bmatrix} p \\ q \\ r \end{bmatrix} \tag{7}$$

$\dot{\phi}\ , \dot{\theta}, \dot{\psi}$ indicates the rate of change of the attitude angle. After completing the construction of these equations, the flight energy conversion efficiency of the UAV must be considered, so a control efficiency equation is constructed as follows to represent the conversion of the quadrotor speed, pull, and torque.

$$f = c_T(\varpi_1^2 + \varpi_2^2 + \varpi_3^2 + \varpi_4^2) \tag{8}$$

$$\begin{cases} \tau_x = dc_T(\frac{\sqrt{2}}{2}\varpi_1^2 - \frac{\sqrt{2}}{2}\varpi_2^2 - \frac{\sqrt{2}}{2}\varpi_3^2 + \frac{\sqrt{2}}{2}\varpi_4^2) \\ \tau_y = dc_T(\frac{\sqrt{2}}{2}\varpi_1^2 + \frac{\sqrt{2}}{2}\varpi_2^2 - \frac{\sqrt{2}}{2}\varpi_3^2 - \frac{\sqrt{2}}{2}\varpi_4^2) \\ \tau_z = c_M(\varpi_1^2 - \varpi_2^2 + \varpi_3^2 - \varpi_4^2) \end{cases} \tag{9}$$

c_T indicates the propeller pull coefficient, c_M indicates the propeller torque coefficient, $\varpi_1,\ \varpi_2,\ \varpi_3,\ \varpi_4$ indicates propeller speed. The parameter matching of QUAV is given in Table.1. The hovering speed is calculated by the equation as follows:

$$\varpi_0 = \sqrt{\frac{mg}{4c_T}} \tag{10}$$

DOI: 10.54254/2755-2721/20/20231076

The mathematical model has been established.

Table 1. QUAV parameter.

Parameter Type	Parameter	Unit
Propeller pull coefficient	0.00001105	/
propeller moment	0.00000017	/
Coefficient	79	*(m/s²)*
Gravity g	0.98066	*(kg*m²)*
X-axis moment of inertia	0.021	*(kg*m²)*
Y-axis moment of inertia	0.022	*(kg*m²)*
Z-axis moment of inertia	0.036	*(kg*m²)*
Total moment of inertia	0.000128	*(kg*m²)*
Pitch d	0.25	*(m)*
QUAV mass	1.8	*(kg)*

3.2. Controller design

The ADRC method was proposed by Han in the last century [10]. It has a theoretical connection with the traditional PID control. However, due to the non-linear and complex mathematical structure of ADRC, its application is limited. Gao et al. proposed a method to linearize ADRC [11], its connection with traditional PID control was established. The quadrotor UAV controller will be designed based on cascaded PID and LADRC.

For a second-order system:

$$\ddot{x} = \ddot{f}(x,\dot{x},t) + b \times u + \sigma(t) = f + b \times u \tag{11}$$

$\sigma(t)$ indicates the disturbance, u and x are the inputs of the system, b indicates the unknown, f is the total disturbance, including external disturbances and internal uncertainties. Select variable $x_1 = x$, $x_2 = \dot{x}$, an equation can be constructed as follows:

$$\begin{cases} \dot{x}_1 = \dot{x} = x_2 \\ \dot{x}_2 = \ddot{x} + f + b \times u \\ x_1 = x \end{cases} \tag{12}$$

The key to LADRC is to estimate the total disturbance of the system by constructing an extended state observer and eliminating it in the controller. So, we need to define an expansion variable $x_3=f$, equation (12) can be rewritten as follows:

$$\begin{cases} \dot{x}_1 = \dot{x} = x_2 \\ \dot{x}_2 = \ddot{x} + f + b \times u \\ x_1 = x \\ \dot{x}_3 = \dot{f} \end{cases} \tag{13}$$

Convert this equation into matrix form as follows:

$$\begin{bmatrix} \dot{x}_1 \\ \dot{x}_2 \\ \dot{x}_3 \end{bmatrix} = \begin{bmatrix} 0 & 1 & 0 \\ 0 & 0 & 1 \\ 0 & 0 & 0 \end{bmatrix} \begin{bmatrix} x_1 \\ x_2 \\ x_3 \end{bmatrix} + \begin{bmatrix} 0 \\ b \\ 0 \end{bmatrix} u + \begin{bmatrix} 0 \\ 0 \\ 1 \end{bmatrix} f \tag{14}$$

$$x = \begin{bmatrix} 1 & 0 & 0 \end{bmatrix} \begin{bmatrix} x_1 \\ x_2 \\ x_3 \end{bmatrix} \tag{15}$$

The equation can be simplified to:

$$\dot{\boldsymbol{X}} = \boldsymbol{A}X + \boldsymbol{B}u + \boldsymbol{E}\dot{f} \tag{15}$$

$$x = \boldsymbol{CX} \tag{16}$$

The observer is designed as:

$$\dot{\boldsymbol{Z}} = \boldsymbol{AZ} + \boldsymbol{B}u + \boldsymbol{K}(x - \hat{x})\boldsymbol{E}\dot{f} \tag{17}$$

$$\hat{x} = \boldsymbol{CZ} \tag{18}$$

In this equation K= (k1 k2 k3). A, B, C, and K are Solved as:

$$\begin{cases} \begin{bmatrix} \dot{z}_1 \\ \dot{z}_2 \\ \dot{z}_3 \end{bmatrix} = \begin{bmatrix} -k_1 & 1 & 0 \\ -k_2 & 0 & 1 \\ -k_3 & 0 & 0 \end{bmatrix} + \begin{bmatrix} 0 & k_1 \\ b & k_2 \\ 0 & k_3 \end{bmatrix} \begin{bmatrix} u \\ x \end{bmatrix} \\ \hat{x} = \begin{bmatrix} 1 & 0 & 0 \end{bmatrix} \begin{bmatrix} z_1 \\ z_2 \\ z_3 \end{bmatrix} \end{cases} \tag{19}$$

State variable observations are z_1, *and* z_2. The total disturbance observation is z_3. Equation (19) can be rewritten as:

$$\begin{cases} \dot{z}_1 = z_2 - (k_1 z_1 - k_1 x) \\ \dot{z}_1 = z_3 - (k_2 z_1 - k_1 x) + bu \\ \dot{z}_1 = -(k_3 z_1 - k_3 x) \end{cases} \tag{20}$$

$$\hat{x} = z_1 \tag{21}$$

The disturbance elimination equation is as follows:

$$u = \frac{u_0 - z_3}{b} \tag{22}$$

Substitute the above equation into equation (11), the equation (22) can be rewritten as:

$$\ddot{x} = f + b\frac{u_0 - z_3}{b} = u_0 \tag{23}$$

Combining the second chapter and adding a PD controller can achieve the QUAV's control. PD control equation is as follows:

$$u_0 = k_p(v - z_1) + k_d z_2 \tag{24}$$

The designed LADRC structure is shown in Figure 4.

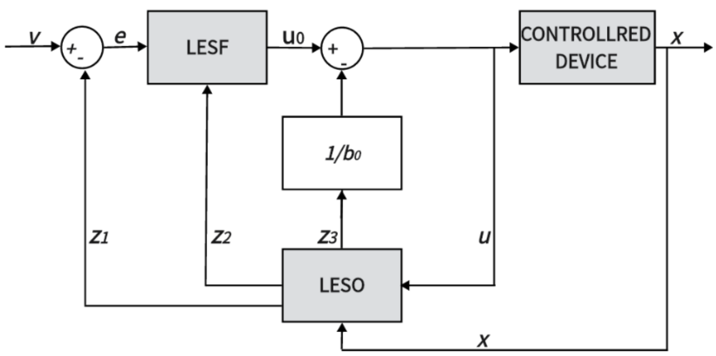

Figure 4. LADRC structure.

Combining the above equations, the total control algorithm of LADRC is as follows:

DOI: 10.54254/2755-2721/20/20231076

$$\begin{cases} \dot{z}_1 = z_2 - (k_1 z_1 - k_1 x) \\ \dot{z}_1 = z_3 - (k_2 z_1 - k_1 x) + bu \\ \dot{z}_1 = -(k_3 z_1 - k_3 x) \\ u = \frac{u_0 - z_3}{b_0} \\ u_0 = k_p(v - z_1) + k_d z_2 \end{cases} \tag{25}$$

The feedback control part of LADRC is like the proportional and derivative parts of PID. The damping factor ξ is introduced to the LADRC system. There are three tuning parameters for linear ADRC, which are the controller bandwidth γ_c, the state observer bandwidth γ_0, and the control variable compensation coefficient b_0. Through the experiment on the model, the LADRC parameters are obtained in table 2.

Table 2. LADRC parameter.

Chanel	γ_c	γ_0	b_0
x	*4*	*5.5*	*-0.35*
y	*20*	*15*	*-0.35*
z	*20*	*8*	*10*
θ	*4*	*1.5*	*0.5*
φ	*15*	*10*	*0.5*
ψ	*8*	*5*	*1*

4. Results of simulation-based performance evaluation

Assuming that there is no disturbance. First, we let the UAV system including the LADRC controller track the signal by setting an ideal ramp forward speed signal, and the result is shown in Figure 5.

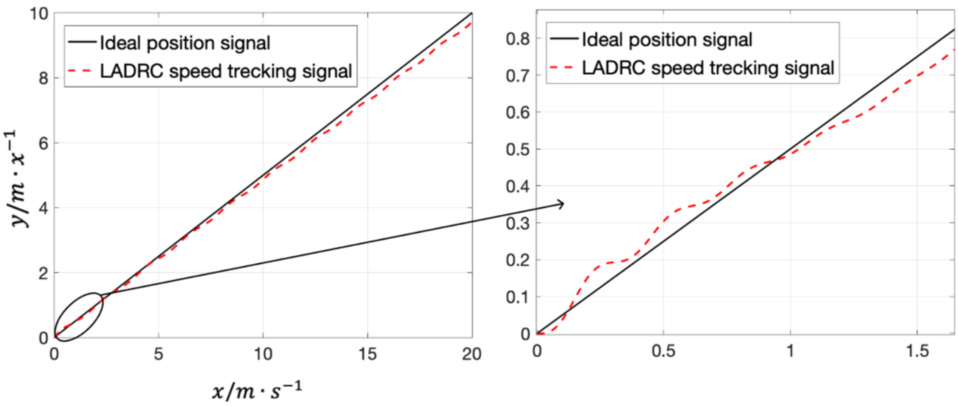

Figure 5. Speed tracking.

The results demonstrate that the controller is capable of high-accuracy tracking of the QUAV at low speeds and low-error tracking at high speeds.

Secondly, we implement the traditional PID according to the content of the second chapter and then implement the LADRC controller according to the content of the third chapter. By comparing the control effects of the two in vertical ascent, the performance of the two is analyzed in Figure 6 and Figure 7. The figures show the vertical altitude change flight and horizontal position change flight of QUAV under semi-ideal conditions. The results show that, in this case, the time for LADRC to reach the desired value for the first time is longer than that of PID control. The rise time, overshoot, settling time, and overall control stability of LADRC are better. To further verify the effect of LADRC control, the performance of LADRC will be verified in various attitudes of the coordinate system. By setting up the coordinate and enter it into the simulation system, we get the expected result and it is shown in Figure 8. The figure shows that with the change of yaw angel, QUAV with the LADRC controller can accomplish stable control. The effect of the LADRC is better than traditional PID.

control.

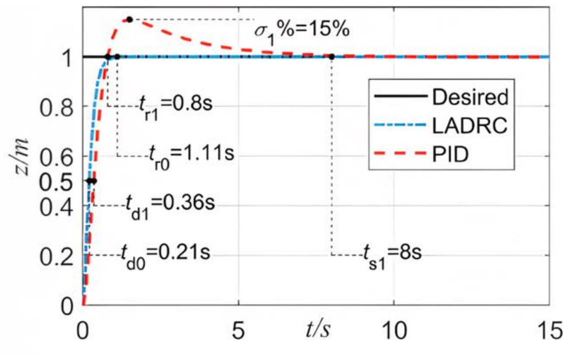

Figure 6. Z-axis take-off experiment.

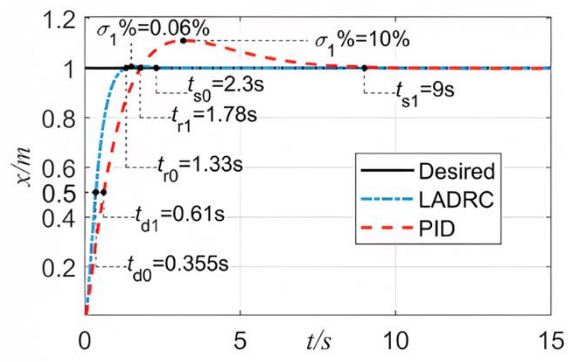

Figure 7. Horizontal displacement experiment.

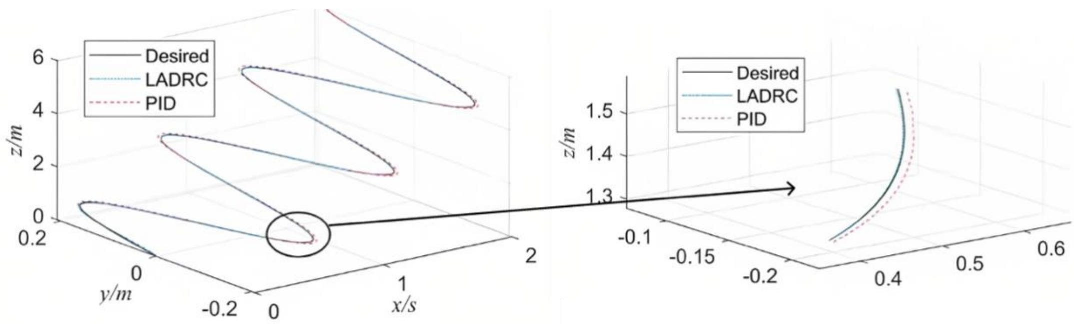

Figure 8. QUAV trajectory tracking.

5. Conclusion

This paper establishes the dynamic model of the quadrotor UAV, completes the design of the control system of the UAV, completes the design of the PID controller and LADRC controller of the UAV, and establishes the Simulink simulation of the UAV control system. In the simulation, in the single-direction flight experiment of the model, the LADRC controller has good response performance such as short delay time, small overshoot, short rise time, and short adjustment time. The simulation experiment verifies the anti-interference performance of the LADRC After the ability, there are still deficiencies in this paper. For example, in the future, based on the existing experimental platform, the controller code of PID and LADRC can be written and burned into the QUAV, and the flight experiment can be carried out to test the anti-interference ability. In the future, QUAV and various UAVs will be more widely used in various fields. In the age of information, QUAV will bring greater convenience to human life.

DOI: 10.54254/2755-2721/20/20231076

References

[1] Dooraki, Amir Ramezani, and Deok-Jin Lee. "An innovative bio-inspired flight controller for quad-rotor drones: Quad-rotor drone learning to fly using reinforcement learning." *Robotics and Autonomous Systems* 135 (2021): 103671.

[2] Karahan, Mehmet, and Cosku Kasnakoglu. "Modeling and simulation of quadrotor UAV using PID controller." *2019 11th International Conference on Electronics, Computers and Artificial Intelligence (ECAI)*. IEEE, 2019.

[3] Islam, Shafiqul, Peter X. Liu, and Abdulmotaleb El Saddik. "Robust control of four-rotor unmanned aerial vehicle with disturbance uncertainty." *IEEE Transactions on Industrial Electronics* 62.3 (2014): 1563-1571.

[4] Priyambodo, Tri Kuntoro, Oktaf Agni Dhewa, and Try Susanto. "Model of Linear Quadratic Regulator (LQR) Control System in Waypoint Flight Mission of Flying Wing UAV." *Journal of Telecommunication, Electronic and Computer Engineering (JTEC)* 12.4 (2020): 43-49.

[5] Noordin, Aminurrashid, et al. "Adaptive PID controller using sliding mode control approaches for quadrotor UAV attitude and position stabilization." *Arabian Journal for Science and Engineering* 46 (2021): 963-981.

[6] Jiang, F., Farhad, P., and Qi, H. "Design, implementation, and evaluation of a neural-network-based quadcopter UAV system." *IEEE Transactions on Industrial Electronics* 67.3 (2019): 2076-2085.

[7] Zhang, X, et al. "Experimental investigation on the online fuzzy energy management of hybrid fuel cell/battery power system for UAVs." *International journal of hydrogen energy* 43.21 (2018): 10094-10103.

[8] Mallikarjunan, Srinath, et al. "L1 adaptive controller for attitude control of multirotors." *AIAA guidance, navigation, and control conference*. 2012.

[9] Åström, Karl J., and Tore, H. "PID control." *IEEE Control Systems Magazine* 1066 (2006).

[10] Han, J. Q. “Auto Disturbance Rejection Controller and It’s Applications.” Control and Decision, Jan. 1998.

[11] Gao, Z. “Scaling and Bandwidth-Parameterization Based Controller Tuning.” Proceedings of the 2003 American Control Conference, 2003., 2005.